Importin-7 mediates memory consolidation through regulation of nuclear translocation of training-activated MAPK in *Drosophila*

Qian Li[a,1], Xuchen Zhang[a,1], Wantong Hu[a,1], Xitong Liang[b,1,2], Fang Zhang[a], Lianzhang Wang[a], Zhong-Jian Liu[c,d], and Yi Zhong[a,3]

[a]Tsinghua-Peking Center for Life Sciences, McGovern Institute for Brain Research, Ministry of Education Key Laboratory of Protein Sciences, School of Life Sciences, Tsinghua University, Beijing 100084, China; [b]School of Life Sciences, Peking University, Beijing 100871, China; [c]Shenzhen Key Laboratory for Orchid Conservation and Utilization, National Orchid Conservation Center of China and Orchid Conservation and Research Center of Shenzhen, Shenzhen 518114, China; and [d]Center for Biotechnology and Biomedicine, Graduate School at Shenzhen, Tsinghua University, Shenzhen 518055, China

Translocation of signaling molecules, MAPK in particular, from the cytosol to nucleus represents a universal key element in initiating the gene program that determines memory consolidation. Translocation mechanisms and their behavioral impact, however, remain to be determined. Here, we report that a highly conserved nuclear transporter, *Drosophila* importin-7 (DIM-7), regulates import of training-activated MAPK for consolidation of long-term memory (LTM). We show that silencing DIM-7 functions results in impaired LTM, whereas overexpression of DIM-7 enhances LTM. This DIM-7–dependent regulation of LTM is confined to a consolidation time window and in mushroom body neurons. Image data show that bidirectional alteration in DIM-7 expression results in proportional changes in the intensity of training-activated MAPK accumulated within the nuclei of mushroom body neurons during LTM consolidation. Such DIM-7–regulated nuclear accumulation of activated MAPK is observed only in the training specified for LTM induction and determines the amplitude, but not the time course, of memory consolidation.

long-term memory | consolidation | *Drosophila* | importin | MAPK

Nuclear translocation of behaviorally activated signaling molecules is widely reported to be essential for formation of protein synthesis-dependent long-term memory (LTM) from invertebrates to vertebrates, suggesting a universal principle underlying memory consolidation (1–3). Extensive efforts have been devoted to determining how such signaling molecules activate the genetic program for memory consolidation through modulation of transcription factors, epigenetic components, or other mechanisms (4–7). However, it is still not clear how training-activated signaling molecules, such as mitogen-activated protein kinase (MAPK), are imported into the nucleus and how such transporting mechanisms impact memory consolidation (8–12).

MAPK (ERK in this case) exceeds the size limit for passive diffusion through nuclear pores and must be transported by either facilitated diffusion, which is energy independent, or active import (13, 14). Recent studies indicate that activated MAPK can be transported actively over a long distance from the synapse to nucleus in hippocampal neurons in response to stimulation (15, 16). The classic active import of proteins is mediated via a family of transport receptors, importin α and β, in the form of heterodimers, but the cargos must have the nuclear localization signals (NLSs) (17). Indeed, there are reports of effects of such classic translocation mechanisms on synaptic plasticity (18, 19). Owing to lack of the identified NLSs, MAPK translocation needs to bind with an adaptor that contains NLSs or go via a noncanonical route, β-like importin-dependent translocation (20). β-Like importin-7 is known to be capable of nuclear importing of activated MAPK in both *Drosophila* and vertebrates (21, 22). This translocation plays a pivotal role in the development of wings, eyes, and the myotendinous junction in *Drosophila* (23–25). Here, we report that *Drosophila*

importin-7 (DIM-7) plays an essential role in the regulation of training-activated MAPK for memory consolidation.

Results

DIM-7 Regulates Long-Term Memory Bidirectionally. We first determined whether DIM-7, encoded by the moleskin (*msk*, CG7935) gene, plays any role in memory formation. The memory components assayed include single-trial-training–induced immediate short-term memory; massed-training–induced 24-h memory, which includes presumably only anesthesia-resistant memory (ARM); and spaced-training–induced 24-h, 48-h, and 4-d memory, including mainly protein-synthesis–dependent LTM with the condition reported here. These memory components were measured using a well-defined aversive classical conditioning paradigm of pairing an odor with foot electric shock (26). To minimize effects of developmental abnormality (homozygous lethal for *msk* mutants), an inducible expression system (*hsGAL4*; Fig. S1A) was used to manipulate expression levels of DIM-7. Acute RNAi-dependent down-regulation of DIM-7 expression (*hsGAL4/UAS-msk-RNAi*) did not affect the single-trial–induced immediate memory (Fig. 1A, *Left*) or the massed-training induced 24-h ARM (Fig. 1A, *Middle*). In contrast, the spaced-training induced 24-h LTM was attenuated significantly (Fig. 1A, *Right*). We confirmed the observed phenotype by using two other independent RNAi lines (Fig. S2A). Conversely, acute overexpression of DIM-7 (*UAS-msk/+*;

Significance

Nuclear import of training-activated signaling molecules is an essential step in initiating memory consolidation. As importin-dependent nuclear translocation is reported in regulation of long-term synaptic plasticity, the current work identified the *Drosophila* homolog of vertebrate importin-7 (DIM-7), in determining consolidation of the protein synthesis-dependent long-term memory (LTM). The amount of DIM-7 expressed determines the level of LTM consolidated and the level of accumulation of behavioral-activated MAPK within the nuclei of mushroom body neurons. Thus, only training that produces LTM could activate DIM-7–dependent pMAPK translocation for initiating memory consolidation.
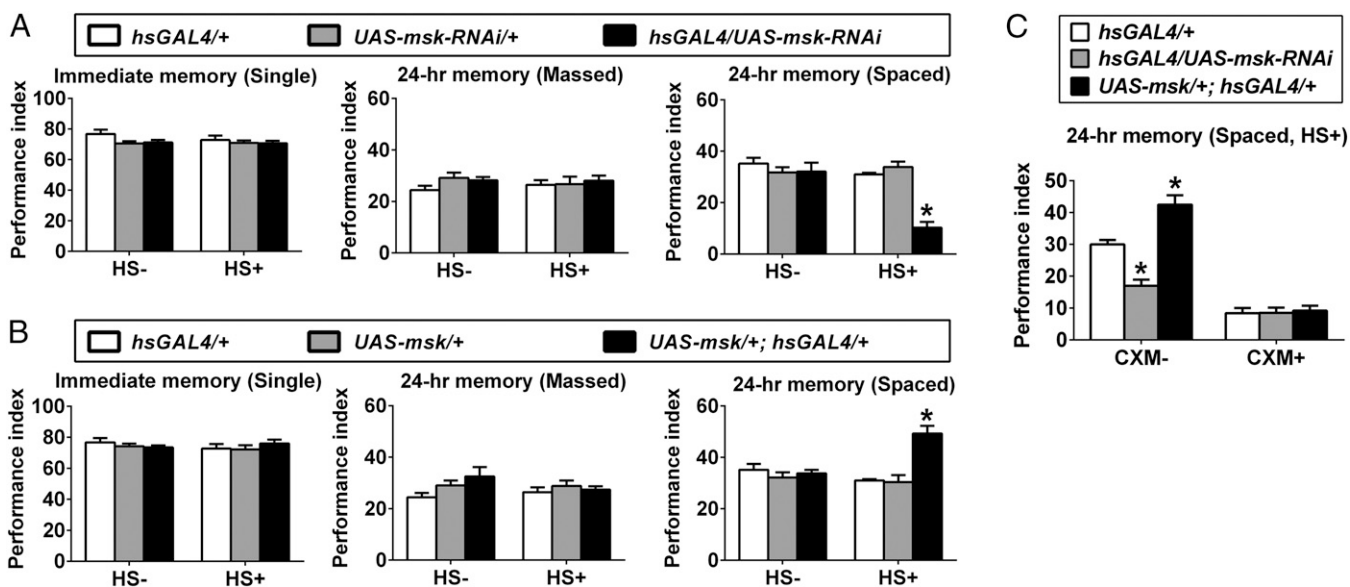
Fig. 1. DIM-7–dependent bidirectional regulation of LTM formation. (*A*) Attenuated spaced-training–induced 24-h memory by RNAi knockdown of DIM-7 expression. Genotypes are as described (*Top*). Acute expression was induced by the heat-shock (HS+) treatment. No heat shock (HS−) served as a control. In all figures, immediate memory was induced after single-trial training (single), 24-h ARM by massed training (massed), and 24-h LTM by spaced training (spaced). (*B*) Enhanced spaced-training–induced 24-h LTM due to acute overexpression of DIM-7. Similarly, immediate memory (*Left*) and ARM (*Middle*) were not affected. (*C*) Feeding of protein synthesis inhibitor, CXM, blocked LTM formation and DIM-7 effects. Bars, mean ± SEM (*n* = 8); *P < 0.05.

hsGAL4/+) enhanced the amplitude of spaced-training–induced 24-h memory, also without affecting immediate memory and ARM (Fig. 1*B*). The affected memory component is indeed protein-synthesis–dependent LTM, as feeding of a protein synthesis inhibitor, cycloheximide (CXM) (26), abolished the spaced-training–induced 24-h memory as well as the effects of DIM-7 (Fig. 1*C*).

DIM-7 Affects Consolidation Stage of Long-Term Memory in Neurons. A panneuronal gene-switch expression system (*elav*-GS; Fig. S1*A*) (27, 28) was used to show that acute down- or up-regulation of DIM-7 expression within neurons is sufficient to produce impairment (*elav-GS/UAS-msk-RNAi*) or enhancement (*UAS-msk/+; elav-GS/+*) of LTM (Fig. 2*A* and Fig. S2*B*). The observed change of 24-h memory occurred after the spaced training but not the single-trial training (Fig. S2 *C* and *D*).

LTM consists of acquisition, consolidation, and maintenance until retrieval sequentially (2, 29). With the help of this panneuronal-inducible driver, we determined the time window within which DIM-7 is required for LTM formation. The phenotypes of the 24-h LTM could be observed when up- or down-regulation of DIM-7 expression was induced within a time window of 48 h that spans either before (24 h) plus after (24 h) training, or only after (24 h) training (Fig. 2*A*). This showed that DIM-7 is involved after memory acquisition. To separate consolidation from retrieval, 48-h as well as 4-d LTM was assayed. The first 24-h induction (consolidation period) of up- or down-regulation of DIM-7 expression after spaced training was sufficient to produce expected LTM phenotypes for 48-h memory (Fig. 2*B*, B1) and even 4-d memory (Fig. S3*A*). In contrast, induction in the last 24 h (retrieval period) before testing the 48-h memory failed to cause any significant behavioral effects (Fig. 2*B*, B2). In fact, the first 12-h induction, but not the last 12-h induction, was capable of producing the observed LTM phenotypes (Fig. S3*B*). RU486 feeding for only 7.5 h is sufficient to induce significant overexpression of targeted protein (27). Consistent with this report, our Western blot result indicates that a significant level of overexpressed YFP-tagged DIM-7 was detected with an 8-h induction period (Fig. S4*C*). YFP-tagged DIM-7 maintains DIM-7 functions (Fig. S4*A*) (23) and was used extensively in the later part

of the experiments described in this paper. Thus, DIM-7 affects LTM in the period of consolidation.

DIM-7 Regulates Long-Term Memory in Mushroom Body Neurons. The mushroom body (MB) is widely reported as the pivotal area for olfactory LTM formation in *Drosophila* (30–35). Two lines of evidence presented below support the idea that DIM-7 functions are confined to MB neurons for the observed behavioral effects. First, manipulation of DIM-7 expression produced an expected impairment or enhancement of memory consolidation (Fig. 3*A* and Fig. S4*B*), when targeted to MB neurons through
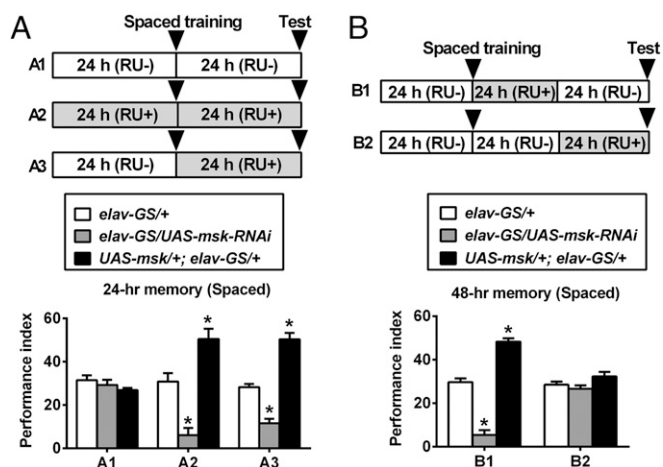

Fig. 2. DIM-7 regulates LTM during consolidation. (*A*) The time window for DIM-7 effects is confined to the period after completion of spaced training. The drug (RU486) feeding (RU+ vs. RU−) regimens are depicted (*Top*). Genotypes are shown in the *Middle*. Spaced-training–induced 24-h LTM is presented in the *Bottom* of the histogram. RU486 feeding (RU+) after training (A3) was sufficient to affect 24-h LTM. (*B*) Effective within the period of consolidation. For 48-h LTM, RU486 feeding (RU+) was sufficient in the first 24 h after spaced training (B1), but insufficient in the last 24 h (for retrieval; B2). Bars, mean ± SEM (*n* = 8); *P < 0.05.

RU486-inducible MB-specific GAL4 (Fig. S1*A* shows expression pattern of MB-GS) (36). Second, manipulation of DIM-7 expression targeted at brain regions other than the MB neurons failed to produce any significant effects on LTM (Fig. 3*B*). Such expression is achieved through a combination of hsGAL4 with MB-GAL80 (37). hsGAL4 induces altered DIM-7 expression in all tissues, whereas expression of the GAL80 protein in MB neurons suppresses hsGAL4-driven expression (Fig. S1 shows expression pattern of MB-Gal80; hsGal4).

DIM-7 Regulates Nuclear Accumulation of Training-Activated MAPK Within Mushroom Body During Consolidation. The aversive LTM consolidation requires a relatively long time window, which could be revealed through a paradigm of cold-shock anesthesia (26, 38). One might imagine that the more DIM-7 expressed, the faster the nuclear translocation of activated MAPK and so the faster the memory consolidation. To see the time course of memory consolidation, wild-type flies were subjected to a 2-min cold shock at different time points after spaced training and then tested for 24-h memory. Consolidated memory was not affected by the treatment of cold shock. The data show that the most significant period of consolidation was during 12 h after training (Fig. 4*A*). This time course, however, is not significantly altered in flies with over-expression of DIM-7, even though LTM was enhanced (Fig. 4*B*). Thus, alteration in DIM-7 expression regulates the amplitude but not the time course of memory consolidation.

Up to this point, we have shown that DIM-7 played no role in single-trial–induced immediate memory and massed-training–induced ARM, but was specifically involved in the regulation of consolidation of spaced-training–induced LTM. Now we needed to address whether the specific role of DIM-7 in memory consolidation results from nuclear transporting of training-activated MAPK, becuse DIM-7 is reported to be a nuclear transporter of activated MAPK (21, 22). For this purpose, immunofluorescence staining of pMAPK in MB neurons was performed at hour 8 after training (Fig. 5) to catch the time window for consolidation as Fig. 4 indicated. Understandably, the pMAPK signal in the cytosol remained largely unaffected by manipulation of DIM-7 expression in naive flies or flies subjected to either massed or spaced training (Fig. S5 *B* and *C*). Thus, pMAPK staining within the calyx, the dendritic area of the mushroom body (Fig. S5*A*), could be used as a constant internal control for scaling the staining intensity.

Viewing the staining images (Fig. 5 *A* and *C*), it can be seen that background signals are present in all nuclei, whereas strong staining signals are limited to a few sparse nuclei. We thus designated two
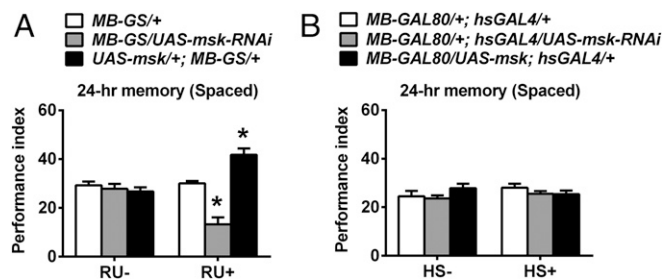
Fig. 4. Dissection of the time course of LTM consolidation. (*A*) Most active period for consolidation occurred in the first 12 h after completion of spaced training. The 24-h LTM was tested without or with 2-min cold shock given at hours 2, 4, 8, 12, or 23, respectively, after training. (*B*) The time course of LTM consolidation was not altered by manipulation of DIM-7 expression. Overexpression of DIM-7 (*UAS-msk/+; elav-GS/+*, RU+) enhanced 24-h LTM, which was disrupted by cold shock at different time points (8 h, 12 h, or 23 h) after spaced training, but did not appear to speed up the time course. Bars, mean ± SEM ($n = 8$); *$P < 0.05$.

parameters: mean intensity ratio, for reflecting the averaged intensity of nuclear accumulation of pMAPK over all MB neurons imaged, and nuclear area ratio, for reflecting the number of nuclei with strong staining that is higher than the intensity in the calyx.

Acute down-regulation of DIM-7 expression exerted no effects on nuclear accumulation of pMAPK in transgenic flies (*elav-GS/msk-RNAi*, RU+) that were either naive or subjected to massed training (Fig. S6 *A* and *B*). Consistent with the behavioral effects, averaged nuclear intensity of pMAPK staining and the number of nuclei with strong staining were significantly reduced in the same transgenic flies but subjected to spaced training (Fig. 5 *A* and *B*), suggesting that a significant role of DIM-7 in transporting pMAPK is confined to the spaced-training condition.

In the case of overexpression of DIM-7, the averaged intensity of nuclear staining of pMAPK was increased as expected in transgenic flies (*UAS-YFP-msk/+;elav-GS/+*, RU+) subjected to spaced training. However, no significant increase was detected in the number of nuclei with strong staining when all MB neurons imaged were included. We then realized that overexpression of YFP-fused DIM-7 without perturbation of its function was not evenly distributed over MB neurons (Fig. S4*D*). Further analysis revealed that nuclei with more accumulation of YFP–DIM-7 showed stronger pMAPK staining in flies subjected to spaced training (Fig. S7). For this reason, our analysis focused on a subgroup of MB neurons with nuclear YFP intensity that was above 70% of the YFP intensity in the calyx. For this group of MB neurons imaged, accumulation of pMAPK was significantly increased in transgenic flies with acute up-regulation of YFP–DIM-7 expression after spaced training. In contrast, nuclear accumulation of pMAPK in the same subgroup of MB neurons remained unaltered in the transgenic flies that were either naive or subjected to massed training (Fig. S6 *C* and *D*). Then we performed additional experiments to further confirm that manipulation of DIM-7 regulates nuclear accumulation of pMAPK in MB neurons during LTM consolidation. First, in flies without manipulating DIM-7, nuclear accumulation of pMAPK in MB, but not its internal control area (optic lobe), was significantly increased at 8 h after spaced training, in contrast to naive and massed conditions (Fig. S8 *A* and *B*). Second, manipulations of DIM-7 within MB neurons affected the nuclear accumulation of pMAPK bi-directionally (Fig. S8*C*). Such data support the idea that DIM-7 contributes to spaced-training–stimulated nuclear accumulation of pMAPK. To strengthen this conclusion, we examined, within the same subgroup of nuclei, the intensity of pMAPK simultaneously with that of YFP–DIM-7. Nuclear distributions of YFP-fused DIM-7 and pMAPK showed a strong positive correlation (Fig. 5*E*),

Fig. 3. DIM-7 dependent regulation of LTM occurs in mushroom body neurons. (*A*) DIM-7 effects on LTM are observed within MB neurons. Genotypes are shown (*Top*). Spaced-training–induced 24-h LTM is presented at the *Bottom* of the histogram. DIM-7 expression is manipulated through RU486-inducible MB-specific tool, MB-GS. No RU486 feeding (RU–) served as a control. (*B*) Ineffective within all neurons outside of the MB region. Such manipulation is achieved through combination of MB-GAL80 with hsGAL4. Manipulation was activated through the heat-shock (HS+) treatment. Bars, mean ± SEM ($n = 8$); *$P < 0.05$.
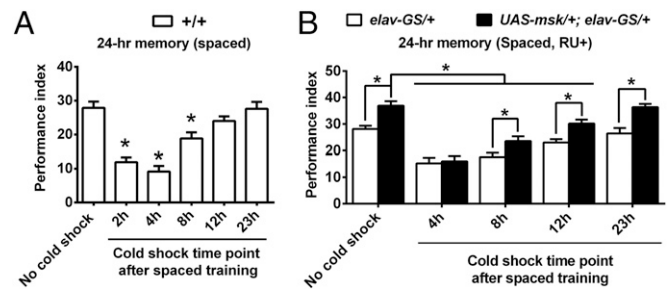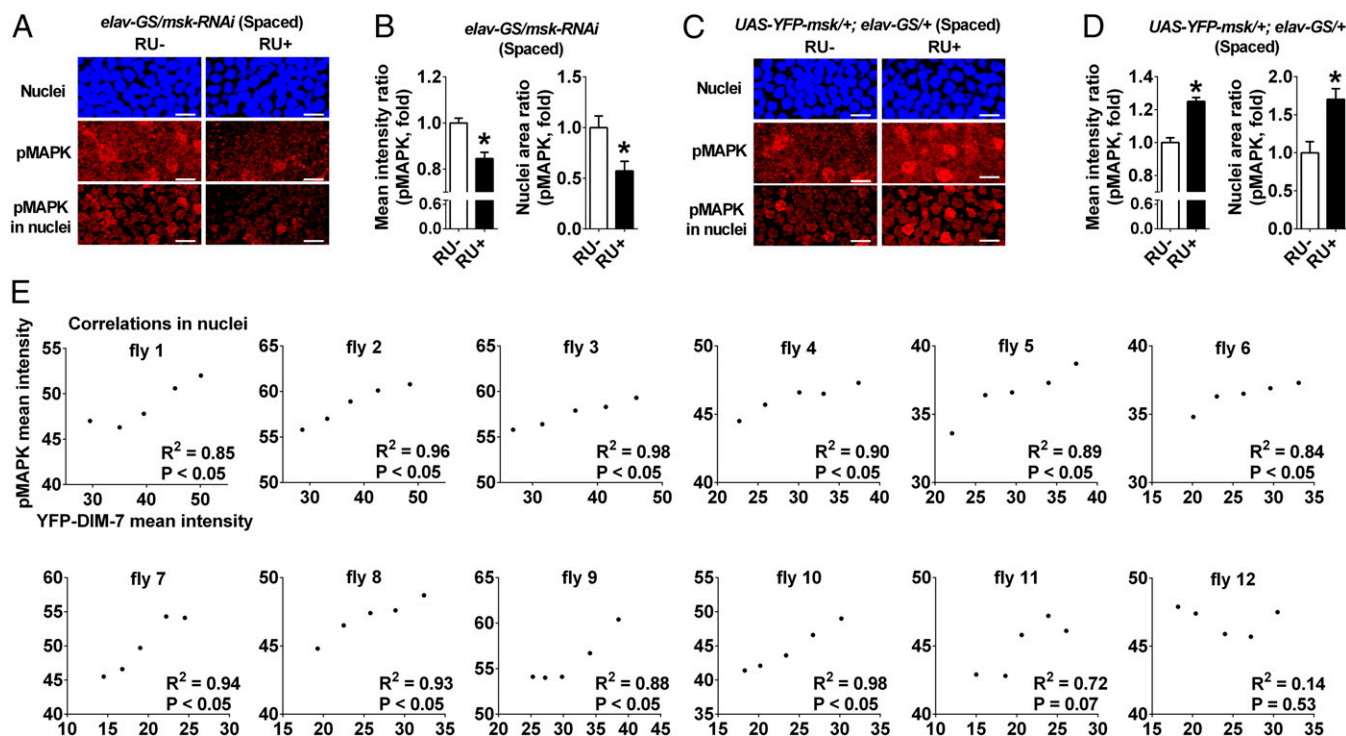
www.manaraa.com

Fig. 5. DIM-7–dependent nuclear accumulation of activated MAPK in mushroom body neurons at hour 8 after spaced training. (*A*) Effects of knockdown (RU+) of DIM-7 expression. Images include nuclear staining (*Top*), pMAPK staining (*Middle*), and nuclear staining of pMAPK (*Bottom*) in control (RU−) and knockdown of DIM-7 (RU+). (Scale bars, 2 μm in all images.) (*B*) Statistical analysis as reflected in mean intensity ratio (averaged intensity of nuclear pMAPK staining) and nuclei area ratio of pMAPK (number of nuclei with strong pMAPK signal). (*C*) Effects of acute overexpression of DIM-7. Images include nuclear staining, pMAPK signal, and pMAPK signal in the nuclei. (*D*) Similar statistical analysis as in *B*. Considering uneven overexpression within the population of MB neurons, only nuclei with sufficient overexpression of YFP-fused DIM-7 (>70% of calyx intensity) are included. (*E*) Correlations between nuclear accumulation of YFP–DIM-7 and pMAPK signals in the same population of MB neurons for individual flies. Twelve flies with overexpression of YFP–DIM-7 (RU+) were randomly picked at hour 8 after spaced training for measurement of nuclear signal intensities of YFP and pMAPK staining. pMAPK signals correlate positively with YFP–DIM-7 signals within the same population of nuclei. Bars, mean ± SEM (n = 7–12); *P < 0.05.

suggesting a major contribution of DIM-7 in spaced-training–induced pMAPK nuclear translocation.

DIM-7–Dependent Regulation of Long-Term Memory Requires MAPK Activation. Finally, several lines of evidence confirm that MAPK activation is indeed critical for LTM formation in *Drosophila*. LTM was impaired with acute knockdown of MAPK targeted to neurons after spaced training in two independent RNAi lines (Fig. 6*A*). In addition, LTM was reduced in a dose-dependent manner with feeding of an inhibitor of MAPK kinase (MEK), U0126, to wild-type flies (Fig. 6*B*). Moreover, feeding of a low dose of U0126 specifically suppressed enhancement of LTM induced by over-expression of DIM-7, even though such a dose did not impair LTM in control flies (Fig. 6*C*).

Discussion

Two major findings emerge from the current study. First, nuclear transporter DIM-7 is involved specifically in regulation of consolidation of protein-synthesis–dependent LTM in MB neurons. This regulation contributes to the amount of memory consolidated, or the amplitude of LTM, but not to the time course of consolidation. Second, the behavioral impact of DIM-7 on LTM requires MAPK activation. Moreover, DIM-7–regulated nuclear accumulation of behaviorally activated pMAPK in the adult fly brain is confined only to spaced training that induces LTM formation during the period of LTM consolidation, whereas DIM-7 has nothing to do with nuclear accumulation of pMAPK stimulated through any other training paradigms that produce memory components other than LTM. These findings lead us to suggest that DIM-7–dependent nuclear translocation of spaced-training–

activated pMAPK is essential in determining the level of LTM consolidated.

DIM-7 was identified as a *Drosophila* homolog of the vertebrate nuclear transporter, importin-7, which belongs to the importin-β superfamily (21, 39). Importins are known to be involved in long-term synaptic plasticity in both invertebrates and vertebrates (18, 40–44). The current work confirms that DIM-7 is indeed critical at the behavioral level in mediating LTM consolidation. We have shown that acute knockdown of DIM-7 impaired LTM, whereas overexpression enhanced LTM. The same genetic manipulations of DIM-7 had no effects on immediate memory and ARM. This behavioral impact was confined to a specific time window of LTM consolidation as well as to a subgroup of brain neurons (MB neurons).

Several experiments were performed to determine whether DIM-7 exerts its effects through mediating nuclear translocation of behaviorally activated pMAPK. DIM-7 is firstly reported to regulate nuclear import of activated MAPK (21) and this function plays important roles in development (23–25). We showed that DIM-7 bidirectionally regulated nuclear accumulation of pMAPK in MB cells during consolidation. More importantly, DIM-7 only affected nuclear accumulation of pMAPK stimulated through training that produced LTM, even though nuclear accumulation of activated MAPK is observed in MB cells of naive flies or of flies subjected to training that produces non-LTM memories. Strong correlation between nuclear accumulation of pMAPK and tagged DIM-7 suggests that nuclear translocation of spaced-training–activated MAPK is mainly mediated through DIM-7. This is also supported by the finding that overexpression of DIM-7, but not MAPK (Fig. S9), enhanced the LTM in *Drosophila*. Although DIM-7 is also reported
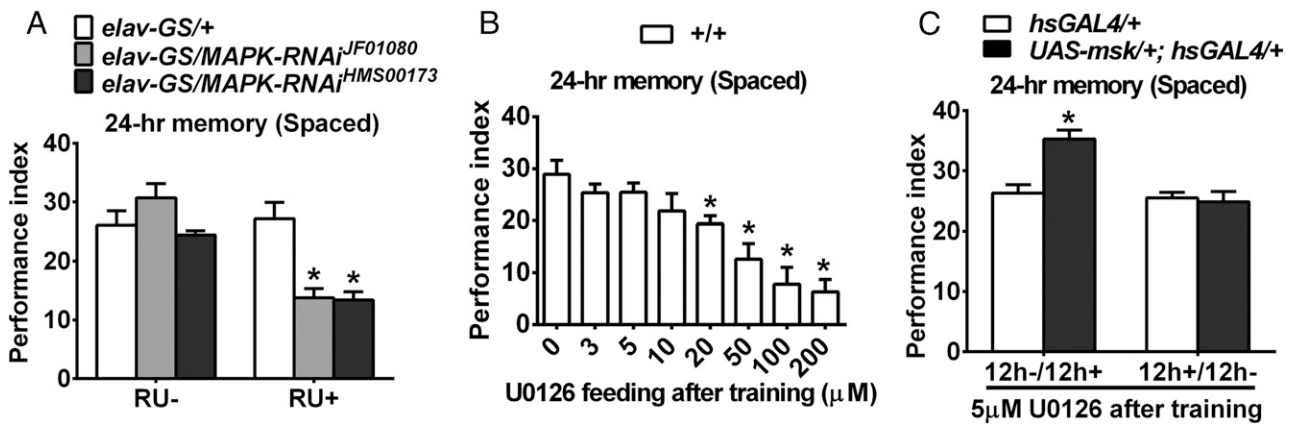
NEUROSCIENCE

www.manaraa.com

Fig. 6. Requirement of MAPK activation during consolidation for DIM-7–dependent LTM enhancement. (*A*) Impaired 24-h LTM by acute down-regulation of MAPK expression. Acute RNAi expression was induced through the GeneSwitch system via feeding of drug RU486 (RU+) after spaced training. Two independent RNAi strains (JF01080 and HMS00173) were used. (*B*) Dosage effects of feeding of a MAPK kinase inhibitor (U0126). Different concentrations were fed after spaced training. (*C*) Specific abolishment of DIM-7–induced enhancement in LTM. To see direct functional link between activation of MAPK and overexpressed DIM-7, flies after spaced training were fed with a low concentration of MAPK inhibitor (5 μM), which does not affect LTM in wild-type flies. Bars, mean ± SEM (n = 6–8); *P < 0.05.

to affect the nuclear import of other cargos, such as Caudal, Mad, and dSNUP (45–47), it remains to be determined whether such translocation contributes to memory consolidation.

It is worth noting that genetic manipulation of DIM-7 affected only the level of LTM consolidation, but appeared not to perturb the time course of consolidation. In *Drosophila*, the time course of olfactory LTM consolidation varies under different training paradigms. Appetitive LTM undergoes rapid consolidation (38), whereas aversive LTM undergoes relatively slow consolidation (34). The time course of memory consolidation and the level of LTM consolidated at each time point after training could be revealed through cold-shock treatment as reflected in Fig. 4. Transgenic flies with acute overexpression of DIM-7 showed a similar time course of consolidation (about 12 h) but a better consolidated memory performance at each time point after hour 2, compared with the control flies. It would be of interest to determine mechanisms underlying the time course of memory consolidation.

Materials and Methods

Fly Stocks. Flies were raised at 25 °C with 60% humidity on standard cornmeal medium in a 12/12-h light/dark cycle. *elav-GS* and *MB-GS* were acquired from Ronald L. Davis, The Scripps Research Institute, Jupiter, FL. *MB-Gal80* was acquired from Scott Waddell, University of Oxford, Oxford. *UAS-YFP-msk* was acquired from Erika R. Geisbrecht, University of Missouri, Kansas City, MO. The following stocks were obtained from the Bloomington Stock Center: *hsGAL4* (BL-1799), *UAS-msk* (BL-23944), *UAS-MAPK-RNAi^JF01080* (BL-31524), *UAS-MAPK-RNAi^HMS00173* (BL-34855), *UAS-MAPK* (BL-32670), *UAS-mCD8::GFP* (BL-5137), and *UAS-nlsGFP* (BL-4776). The following RNAi stocks were acquired from Tsinghua Fly Center: *UAS-msk-RNAi^HMS01408* (THU-1627) (mainly used, described as *UAS-msk-RNAi* in main text), *UAS-msk-RNAi^HMS00020* (THU-0561), and *UAS-msk-RNAi^JF02727* (THU-2735). All strains were outcrossed with 2202U wild-type flies (described as +/+ in all experiments) for at least six generations to equilibrate genetic backgrounds. Specifically, RNAi flies were outcrossed with balancer flies with 2202U wild-type genetic background.

Pavlovian Olfactory Aversive Conditioning. Flies were trained and tested according to standard procedures as described previously (26, 34). Three- to five-day-old flies were used for conditioning in a dark room with 25 °C and 70% relative humidity. 3-Octanol (OCT) (Aldrich, 1.5×10^{-3} in dilution) and 4-methylcyclohexanol (MCH) (Fluka, 1×10^{-3} in dilution) were used as conditioned stimulus (CS), whereas a 60-V electric foot shock (12 1.5-s pulses with 3.5-s intervals) was used as unconditioned stimulus (US). In one cycle training, about 100 flies were subjected to one CS accompanied by US (CS+), and then subjected to the other CS only (CS−). Four cycles were used in massed training (no interval) and spaced training (15-min interval). This paradigm has been used and described previously (35). Flies after massed or spaced training were kept at 18 °C to rest till testing. To test memory, trained flies were transferred to the T maze to choose between CS+ and CS− for 2 min. A preliminary performance index (PI) was calculated as the number of flies avoiding CS+ divided by the total number of flies by percent. A final PI was calculated by averaging two reciprocal groups (one with OCT as CS+, the other with MCH as CS+) to reduce odor bias.

Heat-Shock Regimen. The flies were heat shocked at 37 °C for 40 min and then rested for 2 h at 25 °C until the training began.

Cold-Shock Regimen. The flies were transferred to empty vials in ice for 2 min at planned time point after training and then rested at 18 °C until test.

Drug Feeding. The procedures were described previously (34). Flies were fed with control solution [5% (wt/vol) glucose and 3% (vol/vol) ethanol] in all control groups (CXM−, RU−, or U0126−). For CXM feeding (CXM+), flies were fed with 35 mM cycloheximide (Sigma) dissolved in control solution. For RU486 feeding (RU+), flies were fed with 500 μM RU486 (mifepristone, J&K) dissolved in control solution. For U0126 feeding, according to experimental design, flies were fed with different concentrations of U0126 (Cell Signaling Technology) dissolved in control solution.

Western Blot. Briefly, protein samples were made from 30 fly heads for each time point, run on 10% (vol/vol) SDS/PAGE and transferred to nitrocellulose membrane. Anti-YFP antibody and anti–alpha-tubulin antibody were used as primary antibodies. Anti-rabbit HRP-conjugated antibody was used as secondary antibody. All antibodies were purchased from the Cell Signaling Technology Company. An ECL kit (Millipore) was used for signal detection. The data were quantified by ImageJ software.

Immunofluorescence. Flies were quickly anesthetized on ice and dissected in ice-cold PBS within 5 min. Brains were fixed in 4% (wt/vol) paraformaldehyde in PBS for 30 min on ice. All solutions added after fixation in pMAPK staining were treated with 1% phosphatase inhibitor mixture (Thermo Fisher Scientific). After being washed three times in PBS, brains were treated in blocking solution [PBS with 2% (vol/vol) Triton X-100 and 10% (vol/vol) goat serum] for 60 min at room temperature. Then the brains were transferred into primary antibody solution (PBS with primary antibody, 0.2% Triton X-100, and 1% goat serum) and incubated for at least 24 h at 4 °C. Rabbit anti-pMAPK antibody (1:50, Cell Signaling Technology), mouse anti-nc82 antibody (1:10, DSHB) or chicken anti-GFP antibody (1:2,000, Abcam) was used as primary antibody depending on the experiment. Brains were washed three times again in PBS and transferred into secondary antibody solution (PBS with secondary antibody, 0.2% Triton X-100, and 1% goat serum) and incubated overnight at 4 °C. Goat anti-rabbit IgG Cy3 antibody (1:200, Jackson Immuno-Research), goat anti-mouse IgG Cy3 antibody (1:200, Jackson ImmunoResearch) or goat anti-chicken IgG Alexa Fluor 488 antibody (1:200, Invitrogen) was used as secondary antibody depending on the experiment. Then TO-PRO-3 iodide in diluent buffer (1:500) was used to stain nuclei by incubating for 30 min at room temperature and finally washing with PBS three times. Brains were mounted in

VECTASHIELD mounting medium (Vector Laboratories). Images were taken using confocal microscopy (Zeiss LSM710META).

Quantification of Images. All images used for quantifications were carefully acquired avoiding overexposure or underexposure. For each genotype, data from flies with RU486 feeding (RU+) and flies without RU486 feeding (RU−) were acquired at the same time and under the same microscope parameters. Four to six consecutive slices of each fly, which contained the dendritic region of mushroom body (calyx) surrounded by Kenyon cells, were selected and calculated using Imaris software. Mean intensity of pMAPK in nuclei was divided by that in calyx to get the mean intensity ratio. Area of nuclei overlapped by strong pMAPK signal (judged by intensity above mean in calyx) was divided by total nuclei area. Specifically, in *UAS-YFP-msk/+; elav-GS/+* (RU+) flies, total nuclei area was further selected by intensity of YFP signal. All statistics were calculated from at least six brains. For each genotype, statistics in the induced group (RU+) are shown as fold change compared with the uninduced group (RU−).

Statistics. All data were analyzed using Graphpad Prism 6.0 software. Comparisons between two groups used two-tailed *t* test. Comparisons of multiple groups used one-way ANOVA followed by Bonferroni post hoc comparisons. Statistical significance was shown with *P* value <0.05. All data in bar graphs are shown as means ± SEM.

1. Alberini CM (2009) Transcription factors in long-term memory and synaptic plasticity. *Physiol Rev* 89(1):121–145.
2. McGaugh JL (2000) Memory: A century of consolidation. *Science* 287(5451):248–251.
3. Dudai Y (2004) The neurobiology of consolidations, or, how stable is the engram? *Annu Rev Psychol* 55:51–86.
4. Kandel ER (2001) The molecular biology of memory storage: A dialogue between genes and synapses. *Science* 294(5544):1030–1038.
5. Bading H (2013) Nuclear calcium signalling in the regulation of brain function. *Nat Rev Neurosci* 14(9):593–608.
6. Lee YS, Silva AJ (2009) The molecular and cellular biology of enhanced cognition. *Nat Rev Neurosci* 10(2):126–140.
7. Deisseroth K, Mermelstein PG, Xia H, Tsien RW (2003) Signaling from synapse to nucleus: The logic behind the mechanisms. *Curr Opin Neurobiol* 13(3):354–365.
8. Martin KC, et al. (1997) MAP kinase translocates into the nucleus of the presynaptic cell and is required for long-term facilitation in Aplysia. *Neuron* 18(6):899–912.
9. Sweatt JD (2004) Mitogen-activated protein kinases in synaptic plasticity and memory. *Curr Opin Neurobiol* 14(3):311–317.
10. Thomas GM, Huganir RL (2004) MAPK cascade signalling and synaptic plasticity. *Nat Rev Neurosci* 5(3):173–183.
11. Sindreu CB, Scheiner ZS, Storm DR (2007) Ca2+-stimulated adenylyl cyclases regulate ERK-dependent activation of MSK1 during fear conditioning. *Neuron* 53(1):79–89.
12. Philips GT, Ye X, Kopec AM, Carew TJ (2013) MAPK establishes a molecular context that defines effective training patterns for long-term memory formation. *J Neurosci* 33(17):7565–7573.
13. Wiegert JS, Bading H (2011) Activity-dependent calcium signaling and ERK-MAP kinases in neurons: A link to structural plasticity of the nucleus and gene transcription regulation. *Cell Calcium* 49(5):296–305.
14. Plotnikov A, Zehorai E, Procaccia S, Seger R (2011) The MAPK cascades: Signaling components, nuclear roles and mechanisms of nuclear translocation. *Biochim Biophys Acta* 1813(9):1619–1633.
15. Zhai S, Ark ED, Parra-Bueno P, Yasuda R (2013) Long-distance integration of nuclear ERK signaling triggered by activation of a few dendritic spines. *Science* 342(6162):1107–1111.
16. Karpova A, et al. (2013) Encoding and transducing the synaptic or extrasynaptic origin of NMDA receptor signals to the nucleus. *Cell* 152(5):1119–1133.
17. Perry RB, Fainzilber M (2009) Nuclear transport factors in neuronal function. *Semin Cell Dev Biol* 20(5):600–606.
18. Panayotis N, Karpova A, Kreutz MR, Fainzilber M (2015) Macromolecular transport in synapse to nucleus communication. *Trends Neurosci* 38(2):108–116.
19. Ch'ng TH, Martin KC (2011) Synapse-to-nucleus signaling. *Curr Opin Neurobiol* 21(2):345–352.
20. Flores K, Seger R (2013) Stimulated nuclear import by β-like importins. *F1000Prime Rep* 5:41.
21. Lorenzen JA, et al. (2001) Nuclear import of activated D-ERK by DIM-7, an importin family member encoded by the gene moleskin. *Development* 128(8):1403–1414.
22. Chuderland D, Konson A, Seger R (2008) Identification and characterization of a general nuclear translocation signal in signaling proteins. *Mol Cell* 31(6):850–861.
23. Liu ZC, Geisbrecht ER (2011) Moleskin is essential for the formation of the myotendinous junction in Drosophila. *Dev Biol* 359(2):176–189.
24. Vrailas AD, et al. (2006) smoothened and thickveins regulate Moleskin/Importin 7-mediated MAP kinase signaling in the developing Drosophila eye. *Development* 133(8):1485–1494.
25. Marenda DR, et al. (2006) MAP kinase subcellular localization controls both pattern and proliferation in the developing Drosophila wing. *Development* 133(1):43–51.
26. Tully T, Preat T, Boynton SC, Del Vecchio M (1994) Genetic dissection of consolidated memory in Drosophila. *Cell* 79(1):35–47.
27. Osterwalder T, Yoon KS, White BH, Keshishian H (2001) A conditional tissue-specific transgene expression system using inducible GAL4. *Proc Natl Acad Sci USA* 98(22):12596–12601.
28. Roman G, Endo K, Zong L, Davis RL (2001) P[Switch], a system for spatial and temporal control of gene expression in Drosophila melanogaster. *Proc Natl Acad Sci USA* 98(22):12602–12607.
29. Kandel ER, Dudai Y, Mayford MR (2014) The molecular and systems biology of memory. *Cell* 157(1):163–186.
30. Pascual A, Préat T (2001) Localization of long-term memory within the Drosophila mushroom body. *Science* 294(5544):1115–1117.
31. Pagani MR, Oishi K, Gelb BD, Zhong Y (2009) The phosphatase SHP2 regulates the spacing effect for long-term memory induction. *Cell* 139(1):186–198.
32. Akalal DB, Yu D, Davis RL (2010) A late-phase, long-term memory trace forms in the γ neurons of Drosophila mushroom bodies after olfactory classical conditioning. *J Neurosci* 30(49):16699–16708.
33. Akalal DB, Yu D, Davis RL (2011) The long-term memory trace formed in the Drosophila α/β mushroom body neurons is abolished in long-term memory mutants. *J Neurosci* 31(15):5643–5647.
34. Huang C, et al. (2012) A permissive role of mushroom body α/β core neurons in long-term memory consolidation in Drosophila. *Curr Biol* 22(21):1981–1989.
35. Hirano Y, et al. (2013) Fasting launches CRTC to facilitate long-term memory formation in Drosophila. *Science* 339(6118):443–446.
36. Mao Z, Roman G, Zong L, Davis RL (2004) Pharmacogenetic rescue in time and space of the rutabaga memory impairment by using Gene-Switch. *Proc Natl Acad Sci USA* 101(1):198–203.
37. Krashes MJ, Keene AC, Leung B, Armstrong JD, Waddell S (2007) Sequential use of mushroom body neuron subsets during drosophila odor memory processing. *Neuron* 53(1):103–115.
38. Krashes MJ, Waddell S (2008) Rapid consolidation to a radish and protein synthesis-dependent long-term memory after single-session appetitive olfactory conditioning in Drosophila. *J Neurosci* 28(12):3103–3113.
39. Quan Y, Ji ZL, Wang X, Tartakoff AM, Tao T (2008) Evolutionary and transcriptional analysis of karyopherin beta superfamily proteins. *Mol Cell Proteomics* 7(7):1254–1269.
40. Thompson KR, et al. (2004) Synapse to nucleus signaling during long-term synaptic plasticity; a role for the classical active nuclear import pathway. *Neuron* 44(6):997–1009.
41. Lai KO, Zhao Y, Ch'ng TH, Martin KC (2008) Importin-mediated retrograde transport of CREB2 from distal processes to the nucleus in neurons. *Proc Natl Acad Sci USA* 105(44):17175–17180.
42. Behnisch T, et al. (2011) Nuclear translocation of jacob in hippocampal neurons after stimuli inducing long-term potentiation but not long-term depression. *PLoS One* 6(2):e17276.
43. Jeffrey RA, Ch'ng TH, O'Dell TJ, Martin KC (2009) Activity-dependent anchoring of importin alpha at the synapse involves regulated binding to the cytoplasmic tail of the NR1-1a subunit of the NMDA receptor. *J Neurosci* 29(50):15613–15620.
44. Otis KO, Thompson KR, Martin KC (2006) Importin-mediated nuclear transport in neurons. *Curr Opin Neurobiol* 16(3):329–335.
45. Han SH, et al. (2004) The moleskin gene product is essential for Caudal-mediated constitutive antifungal Drosomycin gene expression in Drosophila epithelia. *Insect Mol Biol* 13(3):323–327.
46. Xu L, et al. (2007) Msk is required for nuclear import of TGF-beta/BMP-activated Smads. *J Cell Biol* 178(6):981–994.
47. Natalizio AH, Matera AG (2013) Identification and characterization of Drosophila Snurportin reveals a role for the import receptor Moleskin/importin-7 in snRNP biogenesis. *Mol Biol Cell* 24(18):2932–2942.

NEUROSCIENCE

Li et al.

www.manaraa.com